Tanzania Journal of Science 50(1): 75-88, 2024
ISSN 0856-1761, e-ISSN 2507-7961

Angular Distribution of *Bremsstrahlung* Spectral Temperature Measured in a Full Dimension of ECR Ion Source Using NaI(TI) Detector

Mwingereza J. Kumwenda
Department of Physics, University of Dar es Salaam, P.O Box 35063, Dar es Salaam, Tanzania
E-mails: kmwingereza@yahoo.com, kmwingereza@udsm.ac.tz
Received 4 Oct 2023, Revised 8 Jan 2024, Accepted 15 April 2024, Published April 2024
https://dx.doi.org/10.4314/tjs.v50i1.6

Abstract

Measurement of angular distribution (AD) of the *bremsstrahlung* spectral temperature from a full dimension of the Electron Cyclotron Resonance Ion Source (ECRIS) along the beam axis is challenging. To overcome some challenges, this paper presents the AD of the *bremsstrahlung* spectral temperature measured in a full dimension of the ECRIS along the beam axis using data obtained from the Busan Center of Korea Basic Science Institute (KBSI). The *bremsstrahlung* spectral temperature from 28-GHz ECR Ion source at the KBSI was measured in six, three, and nine azimuthal angles at the injection, centre, and extraction sides of the ECRIS using three round type thallium-activated sodium iodide (NaI(TI)) scintillation detectors. Monte Carlo simulation based on the Geant4 software package was performed to take the geometrical acceptance and energy-dependent detection efficiency into account due to large non-uniformity in the material budget. True *bremsstrahlung* energy spectra from the 28-GHz ECR ion source were obtained using the inverse-matrix deconvolution method. The unfolding method was based on a full geometry of the Geant4 model of the ECRIS plasma. The results show that in all three measurement locations, the highest value of the spectral temperature was at an angle of 30° coincident with one of the maximum angles of the ECRIS plasma shape.

Keywords: Bremsstrahlung photons; ECRIS; NaI(TI) detectors; Spectral temperature; Plasma shape.

Introduction

The third generation of Electron Cyclotron Resonance Ion Sources (ECRIS) that are operated at a frequency of 28 GHz are of great interest. They are widely used in providing medium to highly charged ion beams, injecting heavy ions into accelerators or studying the interaction dynamics of ions with matter (Bhaskar et al. 2021, Benitez et al. 2022, Thuillier et al. 2022). The beam current dramatically increases when the source is operated at a higher frequency. However, several practical challenges must be overcome before the widespread use of the third generation ECRIS. These technical challenges include; difficulties in fabricating high-field superconducting magnet systems, high-power microwave coupling, plasma chamber cooling, and strong deceleration radiations also known as *bremsstrahlung* from plasma. The ECRIS at Korea Basic Science Institute (KBSI) from which the data of this study were taken was operated within the third generation of the ECRIS range at a frequency of 28 GHz, which produces more intense and energetic *bremsstrahlung* photons (Benitez et al. 2022).

In the ECRIS, bremsstrahlung photons are produced when electrons are decelerated as they interact with another charged particle or nuclei. For the ECRIS this occurs when electrons are decelerated by plasma ions and/or by colliding with a solid surface such as the chamber wall or extraction aperture (Leitner et al. 2006). The bremsstrahlung photons coming from a source form a continuum spectrum and from the inverse of the slope of this spectrum a spectral temperature T_S, is extracted, as described earlier by Benitez et al. 2017. This spectral temperature is related to the hot electron temperature and can be used to assess how changing a source's confining magnetic field affects the hot electron temperature.

Several efforts on the measurement of the bremsstrahlung photons from the ECRIS have been made since the late 1960s (Noland et al. 2010). However, most of these studies measured the bremsstrahlung photons spectra only in one direction, either radially or axially using one or two detectors under different operating conditions (Leitner et al. 2006, Gumberidze et al. 2010, Benitez et al. 2017). However, measurement of the bremsstrahlung photons spectra from ECRIS may require undertaking of AD of the *bremsstrahlung* spectral temperature in a full dimension of the ECRIS along the beam axis. Therefore, this study presents insights into the AD of the *bremsstrahlung* spectral temperature measured in a full dimension of the ECRIS along the beam axis namely the injection, centre, and extraction sides of the ECR ion source. Understanding the *bremsstrahlung* spectral temperature in a full dimension is very important in addressing the performance of the ECRIS superconducting magnetic system.

Materials and Methods

Experimental Setup and Data Acquisitions

The data was measured from the 28-GHz superconducting ECRIS of the compact linear accelerator facility at the Korea Basic Science Institute (KBSI), cyclotron research center. The ECRIS developed at the KBSI is composed of six racetrack hexapole coils and three mirror solenoid magnets. The axial magnetic field is about 3.6 T at the beam injection area and 2.2 T at the extraction region (Park et al. 2016). A radial magnetic field of 2.1 T can also be achieved on the plasma chamber wall. A high current density NbTi wire was selected for winding of sextupole magnet. The inner face of the 5 cm thick solenoid coil is placed at a distance of 44 cm from the beam axis. The 10 cm thick iron shielding structure is 120 cm wide, 122 cm high, and 170 cm long as shown in Figure 1 (Park et al. 2014).

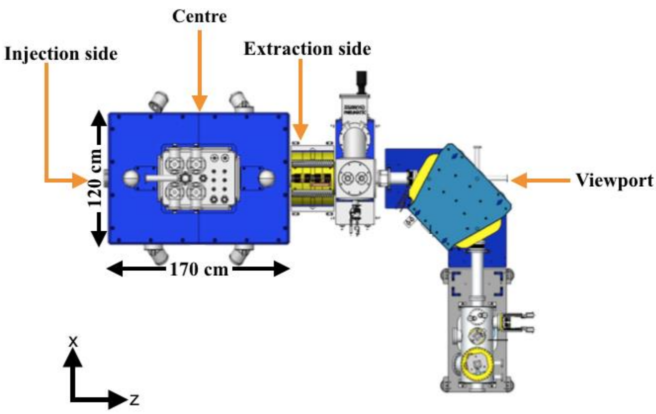

Figure 1: Schematic view of the low-energy accelerator facility at Busan Center of KBSI.

This study has made use of four identical cylindrical NaI(TI) ORTEC 905-3 series detectors. The crystals are optically coupled to the PMT and encased in a light-tight aluminium case. The face of each detector had a diameter of 2 inches by 2 inches with a crystal size of 5.08 cm. The detectors are attached to pre-amplifiers to maintain the time constant of the pulse. The average energy resolution of these detectors is about 7% for full width at half maximum (FWHM) at 662 keV. Each detector has 3 connectors at its rear, high voltage (HV), Anode and Dynode, which are damped by a 50-ohm resistor for this experiment. Both detectors are attached to the pre-amplifiers to maintain the time constant of the pulse.

The experimental setup to measure bremsstrahlung photons spectra in this study was different from the other studies (Leitner et al. 2006, Noland et al. 2010). The inner structure of the ECRIS and the shape of the ECR plasma were taken into consideration in designing this experiment. Photon energy spectra were measured using three round type NaI(TI) detectors as shown in Figure 2 facing the edge of ECRIS. All detectors were labelled with letters D1, D2, D3, and D4 for easy reference, which were operated at +1300 V. The three detectors D1, D2, and D3 were mounted on the support structure for radial measurements, as shown in Figure 2, while the D4 detector was placed at the viewport to monitor the intensity of the ECR plasma.

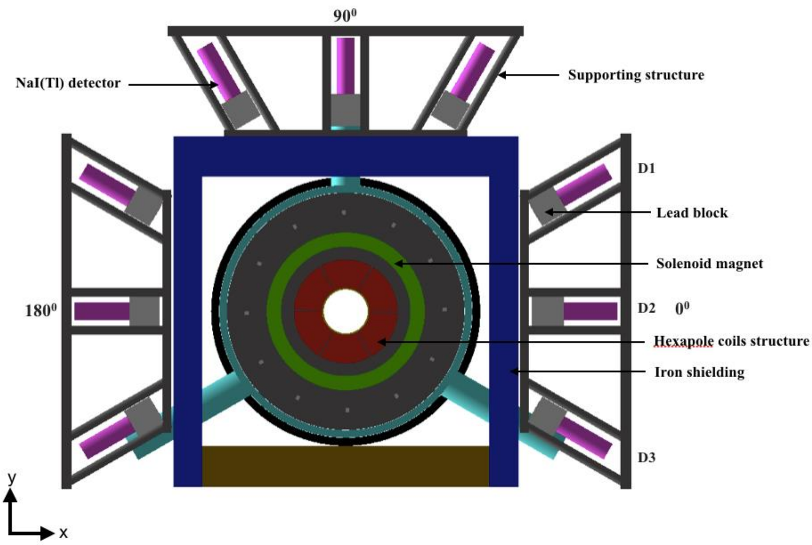

Figure 2: The schematic view of the nine NaI(Tl) detectors at the extraction side.

The bremsstrahlung photons were measured in six, three and nine azimuthal angles at the injection, centre and extraction sides of the ECRIS. At first setup, the three round type NaI(Tl) detectors at the extraction side were placed at the three sides namely right, top and left as depicted in Figure 2. Thereafter, the detector system was moved to the centre (right position only) and lastly moved to the injection side (top and right position). The photon energy was measured at six, three and nine azimuthal angles with 30° intervals at the injection, centre and extraction sides, respectively. The detector face was approximately 2 cm from the iron shielding structure. Each NaI(Tl) detector was placed in a Pb collimator of $100 \times 100 \times 100\ \text{mm}^3$ with a 5 mm hole. The Pb collimator covered a full dimension of the NaI(Tl) crystal. This study presents the results of the bremsstrahlung spectral temperature measured using detector D1 only in all three measurement locations.

NKFADC500 flash ADC which measures input pulse shape was used for data acquisition as illustrated in Figure 3.

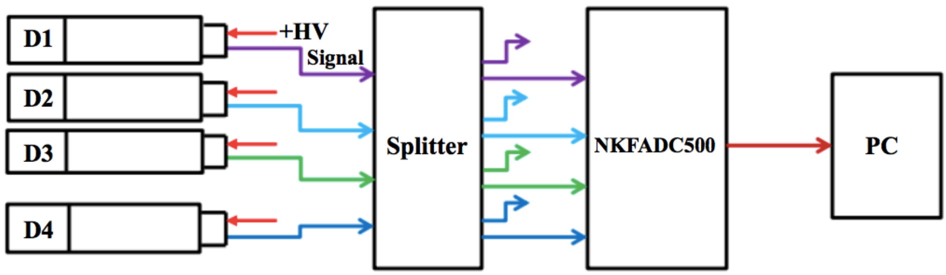

Figure 3: Schematic of an electronic data readout showing the signal from each detector.

The detector signal was fed to the splitting module and then to a 500 MHz FADC and recorded in a coincidence with a reference signal from the detector D4 placed at the viewport. The 4-channel flash ADC module recorded full pulse information from four NaI(Tl) detectors in every 1 μs. Typical pulse shapes are superimposed as in Figure 4.

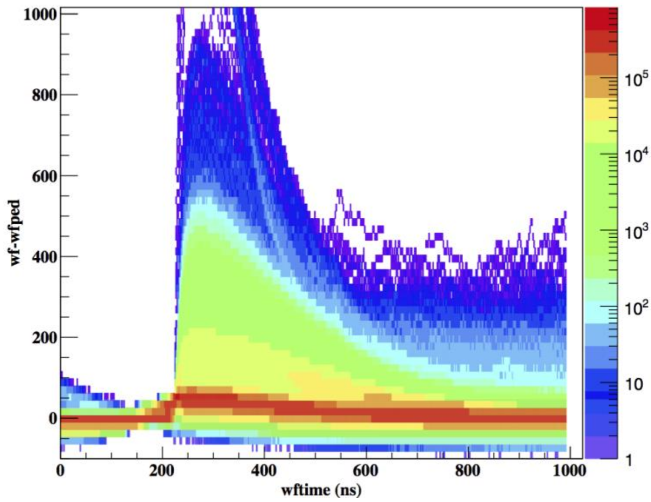

Figure 4: Superimposed NaI(Tl) detector signals digitized using a NKFADC500.

The ring-buffer data were then fed to a DAQ PC. Trigger logic OR provide event triggering condition. Due to the huge data size, the measurement was performed in every 3 minutes. The data recorded by using the NKFADC500 flash ADC were in raw binary form. The raw binary data were decoded to get ROOT format data for analysis (Kumwenda 2018).

DATA ANALYSIS

Energy Calibrations and Background Radiations

During the measurement, the energy calibration of the spectrum was taken using regular radioactive gamma-rays sources namely, ^{60}Co source with gamma-ray energies of 1.173 MeV and 1.332 MeV and ^{137}Cs source with gamma-ray energy of 0.662 MeV (Hajheidari 2016). Then, the three calibrated data points were fitted using a least-squared chi-square linear fit to convert the channel number to its corresponding energy value as shown in Figures 5 (a) and (b).

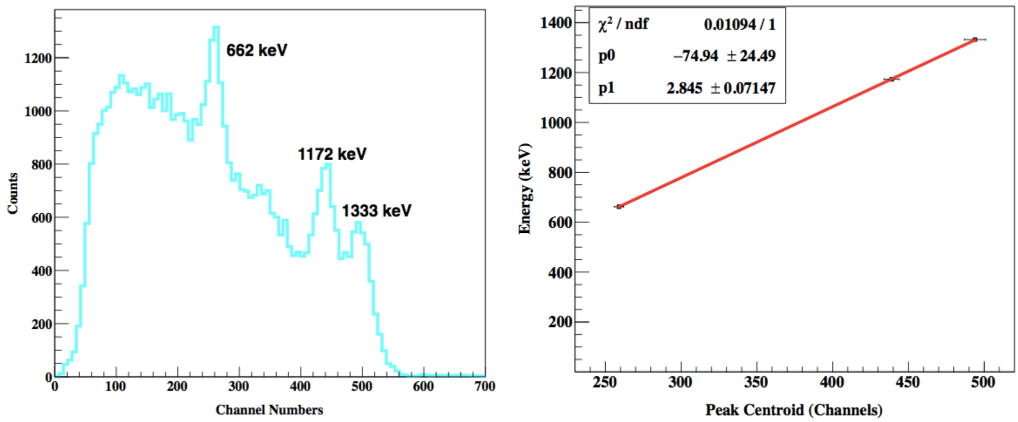

(a) **(b)**

Figure 5: (a) The gamma-ray spectrum of ^{137}Cs and ^{60}Co used for energy calibrations. (b) The energy calibrations for the detectors D1 were used, and all fittings were done using the polynomial function of order one.

The background photon energy spectrum shown in Figure 6 was measured for 10 hours and was normalized with the data taking time and subtracted from the raw spectra for bremsstrahlung photon measurement. In order to take the geometric acceptance and also the energy-dependent detection efficiency into account the Monte Carlo simulation based on the Geant4 package was performed. The simulated efficiencies were used to correct the measured bremsstrahlung photons spectra in all azimuthal angles. Furthermore, all the measured bremsstrahlung photons spectra were normalized to the number of events taken in the same time interval by the detector D4 located at the viewport.

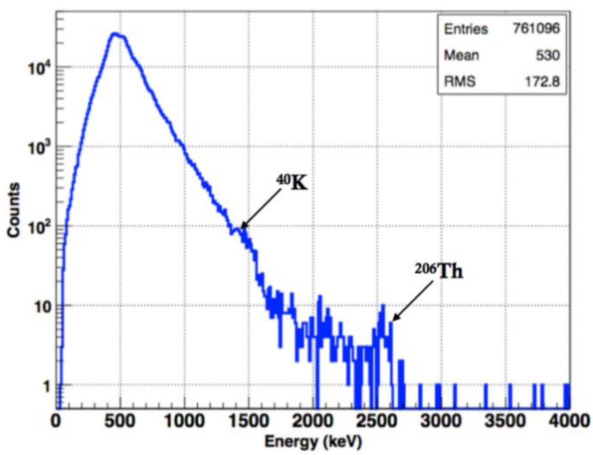

Figure 6: The background photon energy spectrum taken for ten hours.

Direct Matrix Inversion Unfolding Method

The measured spectrum in the physical experiment is usually distorted and transformed by different detector effects, such as finite resolution, limited acceptance, efficiency variations, and perturbations produced by the electronic device. To reproduce the true photon spectrum from the measured distributions it is necessary to consider these effects using response function (Benitez et al. 2008, Thuillier et al. 2022). Normally the response functions are obtained from the response matrix. From the basic mathematical relationship, the measured spectrum $M(E)$ can be calculated using equation (1).

$$M(E) = R(E, E_0)T(E_0) \quad (1)$$

where $T(E_0)$ is the original or true energy distribution of the gamma rays emitted by the source and is the matrix indicating the response function of the detector.

The task is to obtain the true gamma-ray spectrum given the measured energy spectrum. Thus, the desired photon spectrum $T(E_0)$ is calculated from the matrix given by equation (2).

$$T(E_0) = R^{-1}(E, E_0)M(E) \quad (2)$$

where $R^{-1}(E, E_0)$ is the inverse of the response matrix. The pulse height from various mono-energetic gamma-ray spectra was obtained from the Geant4 simulation package based on Monte Carlo using a NaI(Tl) scintillation detector.

Simulation of Response Function

The Monte Carlo method based on the Geant4 package codes was used for the formation of the response matrix. Formation of the response matrix might require more than 100 spectra depending on the dimension of the problem, which is very time-consuming and complicated work (Benitez et al. 2008). To minimize the workload in making the response matrix, this study simulated 200 γ-ray's spectra ranging from 50 to 2040 keV with an interval of 10 keV as represented in Figure 7 in 2D.

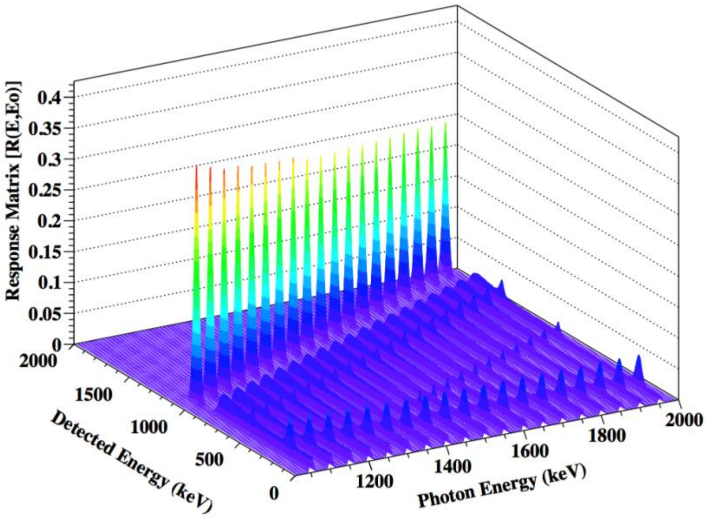

Figure 7: Simulated response function from various mono-energetic gamma rays using NaI(Tl) scintillation detector in 2D.

The z-axis of the 2D spectrum in Figure 7 shows the peak-to-total ratios which gives the diagonal elements of the response matrix. The peak at 200 keV is due to the Compton backscattering as a result of the random direction of the gamma photons during simulation. The other peaks in the y-axis are single and double escape peaks when the gamma photons reach a threshold of 1.02 MeV (Kumwenda 2018).

To acquire valid results, the simulated response function must be obtained with the same conditions as an actual experiment. For the accuracy of the unfolding method defined in equation (1), the response functio should have many energy points (Benitez et al.

2008). The validity of the simulated results was checked by comparing the experimental and simulated spectra as displayed in Figure 8. The comparison of the measured and simulated spectra was done using a radioactive standard gamma source of ^{137}Cs and ^{60}Co.

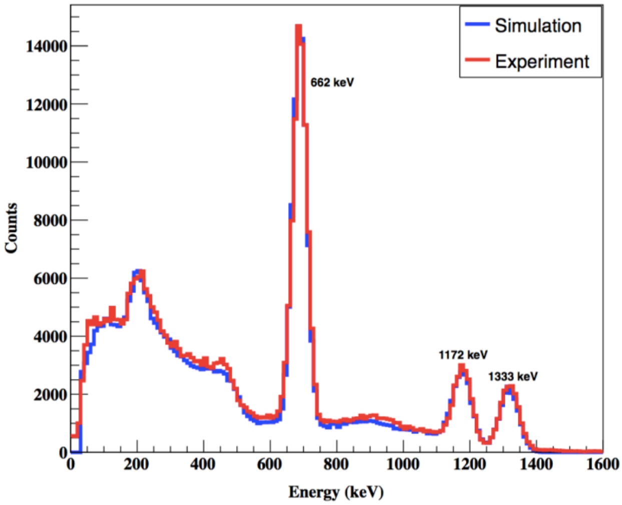

Figure 8: Comparison of experimental and simulated results using standard gamma-ray sources.

It is clear from Figure 8 that, there is a good agreement between the simulated and measured spectra around the photo-peak region, but a slight deviation is observed below 200 keV. The peaks in the simulated and measured profiles at around 200 keV are attributed to the Compton backscattering. It is also observed that the simulated spectra show lower counts between Compton edge and photo-peak that might be caused by the broadening of a single Gaussian function.

Peak to Total Ratio

In a mono-energetic gamma-ray radiation pulse height spectrum, the peak-to-total ratio gives the number of counts contained in the total energy absorption to that contained in the whole spectrum. When a photon with energy, E_0, is radiated there is a certain chance of being fully detected or partially detected. The probability that a photon of energy E_0 is detected with energy E is given by the response matrix . To obtain a response matrix one needs to calculate the Peak-to-Total ratio (P/T) (Almaz and Cengiz 2007, Rahma and Cho 2010). To obtain the peak-to-total ratio, the mono-energetic gamma spectrum peak was fitted to the Gaussian functions, and the peak region was calculated by taking 1.96σ value that makes 95% confidence level for the peak region. The peak region boundary was established as $(\mu - 1.96\sigma, \mu + 1.96\sigma)$ and counts under this region were divided by the total counts of the whole spectrum to get P/T which gives the diagonal elements of the response matrix. To fill in the remainder of the P/T for each photon energy, E_0, was subtracted from the unity and the remainder was shared equally in the energy region between zero and Compton edge. This gives the maximum energy that can be absorbed due to Compton scattering (E_c) given by equation (3).

$$E_c = \frac{2E_\gamma^2}{m_e c^2 + 2E_\gamma} \qquad (3)$$

where m_e is the mass of an electron and E_γ

is the photon energy.

Unfolding Method

In practice, unfolding methods can be divided into two groups, namely, direct and iterative. In this analysis, a brief description of the direct matrix inversion unfolding linear algorithm is presented. The response matrices were arranged in rows and columns to form a M-by-M upper triangular response matrix. The obtained upper triangular matrices $M \times M$ were inverted using the T Matrix class ($TMatrix::kInvert$) in a ROOT software contained in C++ programming language. To obtain vector $M(E)$, the measured spectrum was integrated in a 0.01 MeV energy interval. The multiplication of matrices R^{-1} and column vector M gives another column matrix T , which is the true gamma-ray spectrum of the detector. The acquired column vector T was filled in the histogram and used to plot the true energy spectrum from the measured spectrum. The accuracy of the response matrix was checked by multiplying R and R^{-1} and the results show that all elements along the diagonal are unity while in the inverse matrix, all elements above the diagonal are negative numbers which are physically acceptable (Kumwenda 2020). When the measured spectrum vector M is multiplied by the inverted matrix R^{-1} due to photons of a given energy, the number of photons falls entirely in the channel corresponding to the given energy in the true spectrum for the mono-energetic spectrum.

Validation of Deconvolution Method

Multi-lines Sources (^{133}Cs and ^{60}Co)

Multi-lines and continuous energy spectra were employed to check the reliability of the unfolding software, using Cs-137 and Co-60. It is important to note that Cobalt-60 decays to Nickel-60 via beta-minus emissions, the decay is initially to the nuclear excited state of Nickel-60 from which it emits either one or two gamma rays to reach a ground state of the Nickel-60 isotope (Be et al. 2004). It is known that ^{60}Co has two gamma lines with almost the same probability of emission. Nevertheless, the measured spectrum (Figure 9(a)) shows that the 1.333 MeV line populates much less than the lower line. By application of the deconvolution method both two gamma lines of ^{60}Co (Figure 9(b)) show a similar probability of emission as it expected.

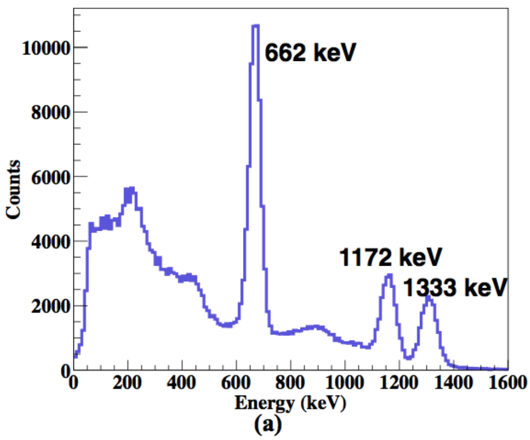

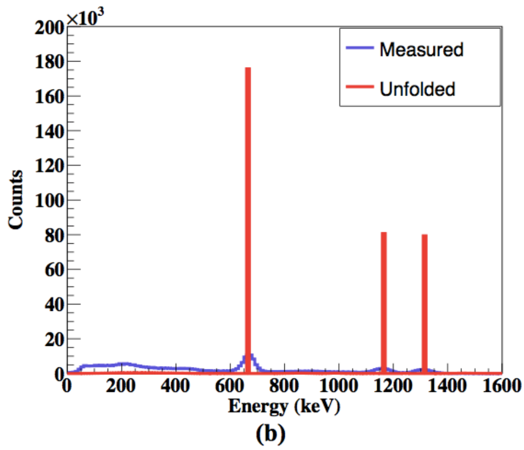

Figure 9: Measured energy spectrum of ^{60}Co and ^{137}Cs and deconvoluted spectrum (Red histogram) using the matrix inversion method.

Strontium (^{90}Sr) Source

^{90}Sr source which emits continuous electromagnetic radiations was also used in checking the trustworthiness of the unfolding software. ^{90}Sr is a radioactive source with a half-life of 28.8 years that decays to Yttrium-90 with a maximum energy of 0.546 MeV. The resulting ^{90}Y undergoes beta decay with a half-life of 64 hours and a maximum energy of 2.3 MeV to stable ^{90}Zr (Romero 2012). Figure 10 shows the measured and deconvoluted spectrum of ^{90}Sr. To unfold ^{90}Sr, 230 γ-ray's spectra ranging between 50 to 2350 keV at an interval step of 10 keV were simulated.

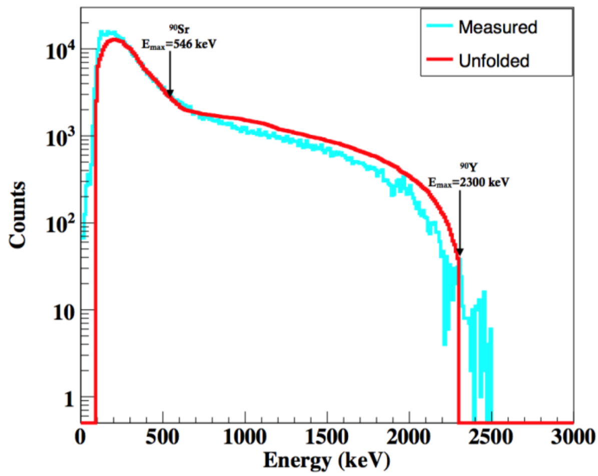

Figure 10: Measured spectrum of a ^{90}Sr source (Cyan) and unfolded spectrum (Red) using the matrix inversion method.

Deconvolution of Bremsstrahlung Photons

The measured spectrum does not directly reproduce the photons spectrum emitted by the electrons that reach the detector. There are numerous processes including attenuation and scattering phenomenologies that can change the recorded spectrum before the photons are recorded in the data acquisition system. Thus, unfolding the measured spectra to get the true spectra is a very crucial step before calibration of the spectral temperature from the ECR plasma. Hence, to obtain correct bremsstrahlung photons spectra from measured ones, the direct matrix inversion deconvolution method was used as explained earlier in the previous subsections. Figures 11 (a) and (b) shows the result of the deconvoluted bremsstrahlung photons spectrum. The number of counts at the end of the high-energy region of the spectrum increases. During unfolding, the starting energy point was set to be 400 keV because in a typical ECRIS, the total material thickness in the radial direction is several tens of millimeters and consists of different elements. Due to the material thickness, the lower energy part of the bremsstrahlung spectrum is largely damped since the radiation penetrates the complicated structure. The threshold selection of 400 keV agreed with the Geant4 simulation of the full geometry of the KBSI ECR ion source. The deconvoluted spectra were overlaid by the red histogram.

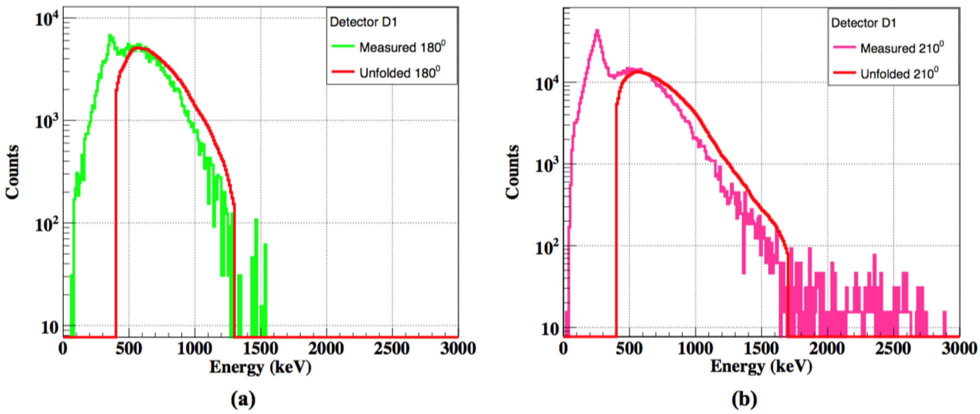

Figure 11: The energy spectra of the Detector D1 (red histogram) obtained after unfolding.

Spectral Temperature Calibration

The elucidation of plasma bremsstrahlung radiation from the ECRIS is commonly done using a spectral temperature Ts. The Ts gives the temperature of the hot electrons in the ECR ion source plasma (Benitez et al. 2017). In the high energy range of the bremsstrahlung photon energy spectra, the spectral power $j(\hbar\omega)$ is assumed to obey the Maxwell-Boltzmann (MB) distribution and hence the spectral power $j(\hbar\omega)$ emitted is proportional to the frequency of the photon given by equation 4;

$$j(\hbar\omega) \propto \exp(-\hbar\omega/kTs) \qquad (4)$$

where $\hbar$ is the Planck's constant, ω is the photon frequency and k is the Boltzmann's constant (Gumberidze et al. 2010). When a semi-log plot of the bremsstrahlung spectrum is fitted with exponential function in the range of photon energies as in Figures 12 (a) and (b), the reciprocal of line's slope gives the spectral temperature Ts in keV. The plots (Figures 12 (a) and (b)) have long energy tail with best line of fit at the energy range between 1400 - 1600 keV with 200 keV energy interval. Consequently, the reciprocal of the line from the data that were measured with the detector D1 at angle 150° and 330° gives the respective bremsstrahlung spectral temperature values of 179.9 keV (Figure 12(a)) and 106.8 keV (Figure 12(b)) which are 180° opposite to each other at extraction side of the ECR ion source as shown in Figures 12 (a) and (b) respectively.

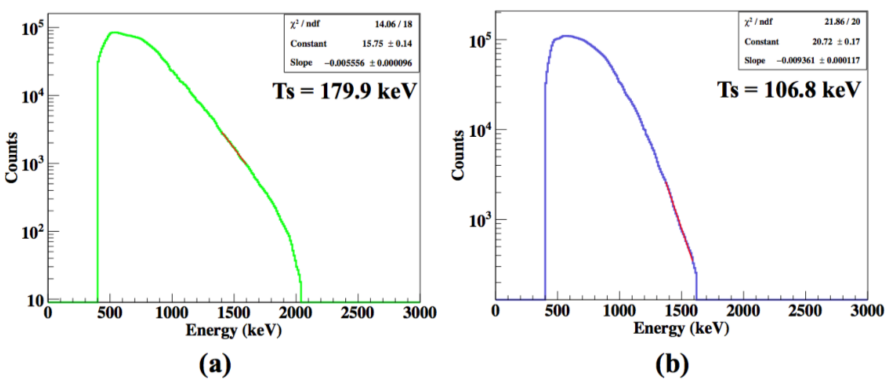

Figure 12: The spectral temperature calibrated from the detector D1 of the sample data measured at angle 150° (a) and 330° (b).

Results and Discussions

The bremsstrahlung spectral temperatures results were calculated from the deconvoluted energy spectra of the measured bremsstrahlung photons after corrections of the detector efficiencies. Figure 13 shows the variations and comparisons of the azimuthal ADs of the bremsstrahlung spectral temperature of the detectors D1 measured in a full dimension at the injection, centre, and extraction sides of the ECR ion source along the beam axis. The results show that the spectral temperature is angular dependent with values ranging between 102 and 234 keV. In comparison, other studies reported the spectral temperature range of between 60 - 200 keV (Leitner et al. 2008, Benitez et al. 2017). Generally, the calibrated spectral temperature gives the direct measure of the temperature distribution of the hot electron in the ECR plasma.

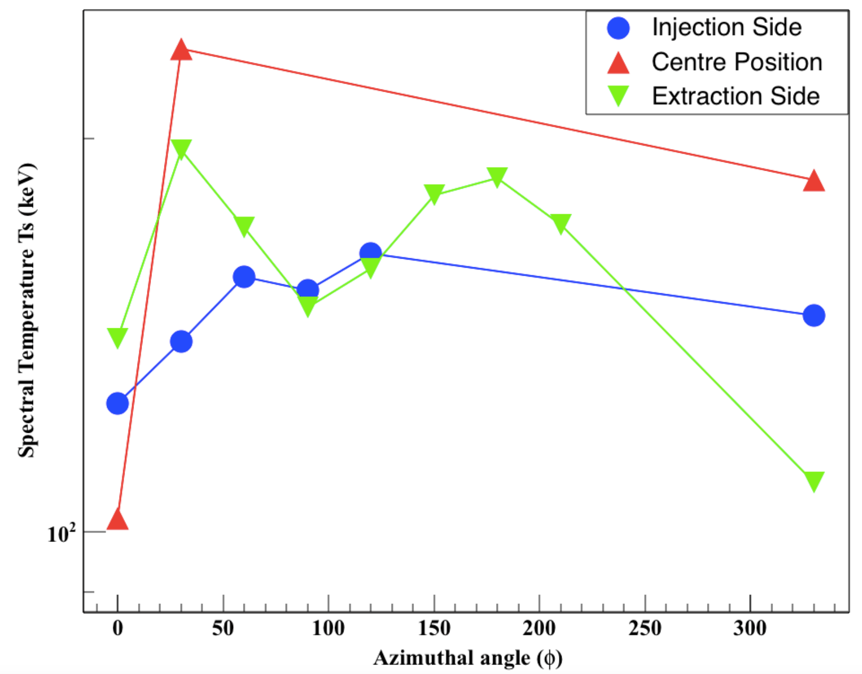

Figure 13: The angular distributions of the bremsstrahlung spectral temperature (T_S) from three measurement configurations.

The ECR plasma was formed in the shape of a twisted triangular prism, due to the sextupole field configuration. The cross-section of the ECR plasma was a triangle at the injection side and an inverted triangle at the extraction side of the ECR ion source in agreement with Mironov et al. 2015. For the injection side, the three corners of the plasma triangle correspond to the angles 90°, 210°, and 330°. Electrons at these corners of the triangles collide with the chamber wall to produce high bremsstrahlung photons and the corresponding high spectral temperatures. The corners at 90° and 330° correspond to two of the maximum angles of the plasma triangle while angle 210° was not accessible during the measurements. However, the maximum value of the spectral temperatures at the injection side of ECR ion source is observed at an angle 120°. The maximum point at 120° cannot be explained by the shape of the ECR plasma. At extraction side, the three corners of the plasma triangle correspond to the angles 30°, 150°, and 270°. The last angle of 270° was not accessible due to the ECR support structure. The corner at

150° with bremsstrahlung spectral temperature of 179.9 keV corresponds to one of the maximum angles. It is interesting to observe that, the maximum spectral temperatures at the extraction side are at an angle of 18 0° and corresponding bremsstrahlung spectral temperature of 163.4 keV cannot be explained by the shape of the ECR plasma. The gaps between the adjacent hexapole coils could account for high spectral temperatures observed at angle 180°.

Furthermore, the maximum value of bremsstrahlung spectral temperature in all three measurement locations was observed at the centre position of the ECR ion source at an angle 30° with a value of 234.5 keV (Table 1). The spectral temperature for detector D1 at an angle 30° is in coincidence with one of the maximum angles of the ECR plasma shape. It is known that the ECRIS plasma at the centre position is formed in the shape the same as the six-arm star due to hexapole magnetic fields (Mironov and Beijers 2009, Mironov et al. 2015). The six corners of the plasma shape correspond to angles 30°, 90°, 150°, 210°, 270° and 330°, which means that after every 60° there should be a maximum angle. During data measurement only three angles 0°, 30° and 330° were involved, other angles were not available due to the ECR support structure. Electrons at two angles namely 30° (234.5 keV) and 330° (186.1 keV) of the hexagon shape at the centre position of the ECR ion source can collide easily with the chamber wall to produce high bremsstrahlung photons, and high bremsstrahlung spectral temperatures. Notably, the minimum spectral temperature of 102.4 keV at an angle 0° was also measured at centre position.

Table 1: Spectral temperatures of the detectors D1 in all three measurement positions.

Azimuthal Angles (ϕ)	Ts (keV) Injection side	Centre position	Extraction side
0°	125.5	102.4	140.5
30°	139.9	234.3	196.1
60°	156.8		171.2
90°	153.2		148.7
120°	163.4		159.1
150°			179.9
180°			186.6
210°			171.9
330°	146.5	186.1	106.8

Conclusions

In this work, the ADs of the bremsstrahlung spectral temperature from the 28 GHz ECR ion source at Busan Center of KBSI were measured in a full dimension along the beam axis using round-type NaI(TI) scintillation detectors. The results show that the maximum spectral temperature in all three measurement locations was at an angle 30° (234.3 keV) which is higher compared to the values of the spectral temperatures reported earlier by Benitez et al. (2017). The implication of this higher spectral temperature value is significant since it suggests that the heating is generally higher at the resonance zone. This result, recommends further work to explore new insights on the design of the magnetic field configuration at the resonance zone in a way that can avoid substantial heat load to the cryostat which resulted in the deterioration of the performance of the ECR ion source.

Declaration of Competing Interest

The authors declare that there is no conflict of interest regarding this work.

Acknowledgements

The author is thankful to the KBSI for hosting the experiments at the KBSI-PNU Laboratory. Appreciation is also extended to Prof. Ahn and Dr. Lee and all members of HANUL research group, at Korea University.

References

Almaz E and Cengiz A 2007 Deconvolution of continuous internal bremsstrahlung spectra of ^{32}P, ^{85}Kr and ^{143}Pr. X-RAY SPECTROMETRY, X-Ray Spectrom. 2007; 36, 419-423.

Be M.M, Chiste V, Dulieu C, Browne E, Chechev V, Kuzmenko, HR, Nichols A, Schonfeld E, and Dersch R 2004 Table of radionuclides, vol. 2. Monographie BIPM-5.

Benitez JY, Noland JD, Leitner D, Lyneis C, Todd DS and Verboncoeur J 2008 High energy component of X-ray spectra in ECR ion sources. *In Proc. ECRIS'08*, Chicago, IL, USA, paper MOPO-08: 77-84.

Benitez J, Lyneis C, Phair L, Todd D and Xie D 2017 Dependence of bremsstrahlung spectral temperature in minimum-B electron cyclotron resonance ion Source. *IEEE Trans. Plasma Sci.* 45(7):1746-1754.

Benitez J, Todd D and Xie D 2022 Studies of bremsstrahlung and characteristics X-ray lines using the VENUS ECR. *J. Phys.* 2244(2022) 012083.

Bhaskar BS, Koivisto H, Tarvainen O, Thuillier T, Toivanen V, Kalvas T, Izotov I, Skalyga V, Kronholm R and Marttinen M 2021 Correlation of bremsstrahlung and energy distribution of escaping electrons to study the dynamics of magnetically confined plasma. *Plasma Phys. Control. Fusion* 63:095010 (17pp).

Gumberidze A, Trassinelli M, Adrouche N, Szabo CI, Indelicato P, Haranger F, Isac JM, Lamour E, Le Bigot EO, Merot J, Prigent C, Rozet JP and Vernhet D 2010 Electronic temperatures, densities and plasma X-ray emission of 14.5 GHz electron-cyclotron resonance ion source. *Rev. Sci. Instrum.* 81: 033303.

Hajheidari MT, Safari MJ, Afarideh H and Rouhi H 2016 Experimental validation of response function of a NaI(Tl) detector modeled with Monte Carlo codes. *J. Instrument.* 11 P06011.

Kumwenda MJ 2018 *Measurements of bremsstrahlung photons in 28 GHz electron cyclotron resonance plasma*. PhD thesis, Korea University.

Kumwenda MJ 2020 Deconvolution of mono-energetic and multi-lines gamma-ray spectra obtained with NaI(Tl) scintillation detectors using direct matrix inversion method. *Tanzania J. Eng. Technol*. 39(2):104-115.

Leitner D, Lyneis CM, Loew T, Todd DS, Virostek S and Tarvainen O 2006 Status report of the 28 GHz superconducting electron cyclotron resonance ion source VENUS. *Rev. Sci. Instr*. 77: 03A302.

Leitner D, Benitez JY, Lyneis CM, Todd DS, Ropponen T, Ropponen J, Koivisto H and Gammino S 2008 Measurement of the high energy component of the x-ray spectra in VENUS electron cyclotron resonance ion source. *Rev. Sci. Instrum.* 79: 033302.

Mironov V, Bogomolov S, Bondarchenko A, Efremov A and Loginov V 2015 Numerical model of electron cyclotron resonance ion source. *Phys. Rev. Special Topics- Accel. Beams* 18: 123401.

Mironov V and Beijers JPM 2009 Three-dimensional simulations of ion dynamics in the plasma of an electron cyclotron resonance ion source. *Phy. Rev. Special Topics – Accelerat. Beams* 12(7): 073501.

Noland J, Benitez JY, Leitner D, Lyneis C and Verboncoeur J 2010 Measurement of radial and axial high energy x-ray spectra in electron cyclotron resonance ion source plasmas. *Rev. Sci. Instrum.* 81: 02A308.

Park JY, Lee BS, Choi S, Kim SJ, Ok JW, Yoon JH, Kim HG, Shin CS, Hong J, Bahng J and Won MS 2016 First results of 28 GHz superconducting electron cyclotron resonance ion source for KBSI accelerator. *Rev. Sci. Instrum*. 87: 02A717.

Park JY, Choi S, Lee BS, Yoon JH, Ok JW, Kim BC, Shin CS, Ahn JK and Won MS 2014 Superconducting magnet performance for 28 GHz electron cyclotron resonance ion source developed at the Korea Basic Science Institute. *Rev. Sci. Instrum*. 85: 02A928.

Rahma MS, and Cho G 2010 Unfolding low-energy gamma-ray spectrum obtained with NaI(Tl) in air using matrix inversion method. *J. Sci. Res. 2* (2), 221-226.

Romero EC 2012 *Optimization of a gas flow proportional counter for alpha decay measurements*, M. Sc. thesis, Universitat Munster.

Thuillier T, Benitez J, Biri S, and Racz R 2022 X-ray Diagnostics of ECR ion sources techniques, results, and challenges. *Rev. Sci. Instrum*. 93: 021102.